Published in final edited form as:
ACS Chem Biol. 2013 April 19; 8(4): 778–788. doi:10.1021/cb300679a.

Peptide ligands for pro-survival protein Bfl-1 from computationally guided library screening

Sanjib Dutta, **T. Scott Chen**, and **Amy E. Keating***
Department of Biology, Massachusetts Institute of Technology, Cambridge, 02139

Abstract

Pro-survival members of the Bcl-2 protein family inhibit cell death by binding short helical BH3 motifs in pro-apoptotic proteins. Mammalian pro-survival proteins Bcl-x_L, Bcl-2, Bcl-w, Mcl-1 and Bfl-1 bind with varying affinities and specificities to native BH3 motifs, engineered peptides and small molecules. Biophysical studies have determined interaction patterns for these proteins, particularly for the most-studied family members Bcl-x_L and Mcl-1. Bfl-1 is a pro-survival protein implicated in preventing apoptosis in leukemia, lymphoma and melanoma. Although Bfl-1 is a promising therapeutic target, relatively little is known about its binding preferences. We explored the binding of Bfl-1 to BH3-like peptides by screening a peptide library that was designed to sample a high degree of relevant sequence diversity. Screening using yeast-surface display led to several novel high-affinity Bfl-1 binders and to thousands of putative binders identified through deep sequencing. Further screening for specificity led to identification of a peptide that bound to Bfl-1 with K_d < 1 nM and very slow dissociation from Bfl-1 compared to other pro-survival Bcl-2 family members. A point mutation in this sequence gave a peptide with ~50 nM affinity for Bfl-1 that was selective for Bfl-1 in equilibrium binding assays. Analysis of engineered Bfl-1 binders deepens our understanding of how the binding profiles of pro-survival proteins differ, and may guide the development of targeted Bfl-1 inhibitors.

Introduction

Interactions among Bcl-2 family proteins play a critical role regulating apoptosis. The family is divided into two major subclasses: (1) pro-survival and (2) pro-apoptotic Bcl-2 proteins. The pro-survival proteins that include Bcl-x_L, Mcl-1, Bcl-2, Bcl-w and Bfl-1 are responsible for antagonizing the activities of pro-apoptotic proteins and thereby inhibiting apoptosis. Among pro-apoptotic proteins, Bax and Bak are downstream effectors of cell death. They form pores in the mitochondrial outer membrane that mediate the release of cytochrome c, with subsequent activation of executioner caspases[(1)]. Another class of pro-apoptotic proteins, the BH3-only proteins, functions to relieve the inhibitory effect of the pro-survival proteins by binding to them[(2)]. Prominent members of this family include the proteins Bim, Bid, Puma, Noxa, Bad, Bmf, Hrk, Bik and Mule. Interestingly, BH3-only proteins exhibit a range of affinities for pro-survival proteins, and disrupting the balance of interacting partners modulates signaling thresholds for apoptosis[(3)].

Pro-survival proteins are frequently over-expressed in cancer cells[(4)]. Bcl-x_L, Bcl-2 and Mcl-1 are attractive therapeutic targets due to their association with aggressive malignant phenotypes and drug resistance to various chemotherapeutic agents[(5, 6)]. However, Bfl-1,

***Corresponding Author** Amy E. Keating 77 Massachusetts Avenue, Building 68-622, Cambridge, Massachusetts 02139, USA Telephone: (617) 452-3398, Fax: 617-852-6143 keating@mit.edu.

SUPPORTING INFORMATION Supplemental Figures 1–7, Supplemental Tables 1–2. This material is available free of charge via the Internet at http://pubs.acs.org.

which has an important function in the hematopoietic system[7, 8], is less well studied. Increased expression of Bfl-1 has been associated with different forms of leukemia and lymphoma[9], and over-expression of Bfl-1 mRNA has been identified in solid tumor tissues of varying origins including breast, colon, lung, ovarian and prostate[10]. In addition, Bfl-1 is associated with metastatic disease in melanoma[11] and hepatocellular carcinoma[12], and RNAi targeting of Bfl-1 along with Mcl-1 in melanoma cell lines leads to enhanced cell death without affecting non-malignant cells[13]. A role for Bfl-1 in tumor progression is indicated by its expression in advanced tumor stages[14]. Furthermore, increased expression of Bfl-1 has been shown to correlate with chemo-resistance in leukemia and breast cancer[15, 16]. These studies highlight the therapeutic potential of Bfl-1 inhibitors[7].

There have been conflicting reports regarding the pro-apoptotic interaction partners of Bfl-1. Bfl-1 has been reported to inhibit cell death associated with Bak activation[17], though the extent of interaction of Bfl-1 with both Bak and Bax is disputed[18–21]. Peptides corresponding to the BH3 motifs of Bim, Puma and Bid, hereafter called Bim BH3, Puma BH3, etc., have been reported to bind tightly to Bfl-1, with dissociation constants of ~50 nM *in vitro*[3, 22]. Binding of the BH3 motif from Noxa, and to a lesser extent the motifs from Bik and Hrk, has also been reported[3, 23]. Interaction with Noxa BH3 and non-interaction with Bad BH3 makes Bfl-1 somewhat similar to Mcl-1 in terms of its BH3-peptide binding profile. In addition, the BH3 mimetic small molecule ABT-737 does not bind tightly to Bfl-1 or Mcl-1, despite having high affinity for Bcl-x_L, Bcl-2 and Bcl-w[23–25]. Therefore, in cells over-expressing Bfl-1/Mcl-1, treatment with ABT-737 only leads to cell death if Bfl-1/Mcl-1 are separately neutralized with other BH3 proteins[3]. A recent study with peptide aptamers identified molecules that bound Bfl-1 and initiated cell-death in lymphoma B-cell lines[26].

Crystal structures of Bfl-1 in complex with peptides corresponding to the BH3 motifs of pro-apoptotic proteins show a conserved binding mode shared with other pro-survival family members[18, 27, 28]. A surface groove on Bfl-1 engages an amphipathic BH3 helix of ~16 – 25 residues. Positions on the BH3 helix, which follow a loose 7-residue hydrophobic/polar repeat, are often designated a – g, as shown for a peptide derived from Bim binding to Bfl-1 in Fig. 1a and b. There are differences in the binding groove of Bfl-1 compared to other family members. For example, Bfl-1 has a highly atypical glutamate residue at a position that is typically occupied by valine or leucine in other pro-survival proteins. This contributes to making the Bfl-1 groove slightly negatively charged, in contrast to the groove of Mcl-1, which is slightly positively charged[27–29]. Overall, the sequence identity between Mcl-1 and Bfl-1 is only 21.4%, and the similarity with other pro-survival proteins is even lower.

Despite an emerging appreciation of the importance of Bfl-1, a good understanding of its BH3-binding specificity is lacking. In this study, we isolated high affinity BH3-like peptides that bound to Bfl-1 by screening a combinatorial peptide library that was computationally designed based on published experimental data. Combining screening and rational design, we identified a peptide that bound tightly to Bfl-1 in preference to interacting with pro-survival proteins Bcl-x_L, Bcl-2, Bcl-w and Mcl-1. Mutational and structural analyses highlighted positions important for preferential binding.

Results and Discussion

Computational library design

We based our peptide designs on the BH3 region of human Bim, which is reported to bind strongly to Bfl-1 (Fig. 1a, b)[3, 18, 22]. Although the BH3 region of Noxa interacts preferentially with Mcl-1 and Bfl-1 over Bcl-x_L, Bcl-w and Bcl-2, potentially making it an appealing starting point for design, Noxa BH3 binding to Bfl-1 is weaker than that of Bim

BH3[3, 18]. Furthermore, SPOT array binding data are available for hundreds of point mutants of Bim BH3, and we chose to use these data to guide our design procedure[30–32]. An image of a Bim BH3 substitution SPOT array probed with 100 nM Bfl-1 is shown in Fig. 1c[32]. Based on such array data for Bim BH3 point mutants, we developed position specific scoring matrices (PSSMs) for predicting the binding of BH3-like peptides to all five proteins[31, 32]. For example, model $PSSM_{Bfl\text{-}1}$, derived from the data in Fig. 1c, can be used to score binding of BH3-like peptides to Bfl-1. We developed a computational approach guided by the PSSM models to design a combinatorial library enriched in sequences predicted to bind tightly and selectively to Bfl-1.

In the first step of library design (Fig. 1d), we defined two classes of mutations: non-disruptive and specific. A single-residue substitution was defined as non-disruptive if its Bfl-1 PSSM score was among the top 50% of the Bfl-1 binding scores for all amino acids across all positions tested. A non-disruptive mutation was further classified as specific if it was ranked in the top 33% of mutations that favored binding to Bfl-1 over another pro-survival protein (see Methods). Four types of specificity mutations (Bfl-1 over Bcl-x_L/Mcl-1/Bcl-2/Bcl-w) were defined (Table 1). Substitutions at positions 2d, 2e, 2g, 3a, 3d, 3g and 4a (Fig. 1a and b) met our criteria for being specific and non-disruptive, therefore, we constructed our library using a set of degenerate codons to maximize diversity at these positions (see Methods).

The diversity of the optimized library, which had a theoretical size of 8.9×10^6, is shown in Table 1. It covered 67% of predicted specific mutations and 55% of predicted non-disruptive mutations, as well as the wild-type residue at each position. We compared our Bfl-1-targeted library to a Bim BH3-based library that was previously designed by hand using general structural and chemical principles. The later lacked any intentional bias towards any pro-survival protein[31]. The computationally designed library exhibited improved PSSM scores for Bfl-1 (Fig. 1e – h), as expected. Compared to the previously designed library, more sequences were identified with higher Bfl-1 PSSM scores and lower Mcl-1 (Fig. 1e) or Bcl-x_L (Fig. 1f) PSSM scores. Only a few residues were predicted to impart specificity for Bfl-1 over Bcl-w and Bcl-2, so the difference between the two library PSSM score distributions was modest for these proteins (Fig. 1g and h).

Previous studies showed that a PSSM model based on SPOT array intensities performed well at predicting sequences specific for either Bcl-x_L or Mcl-1[31]. However, errors associated with synthesis and array processing, and the simple additivity assumptions of PSSMs, limit the predictive power of such models. Therefore, our library design strategy was guided by the model but not tightly constrained by it. For example, only a few mutations were predicted to confer specificity for Bfl-1 over Bcl-w. One design strategy would be to require that at least one of these residues be included in all library members, but this could be risky without verification of the influence of these residues on binding. Instead, we identified all substitutions predicted to confer specificity against any of the four off-target receptors, and required only that the library encode at least one specificity residue of each type. We reasoned that this would maximize the diversity of available specificity strategies, and the screening could identify good combinations. Even if no predictions were correct for one or more particular binary specificity class (e.g. Bfl-1 over Bcl-w), as long as other specificity predictions were accurate the library would still be sampling a useful sequence space.

Library screening for peptides that bind Bfl-1—We used yeast-surface display to identify Bfl-1-binding peptides (Fig. 2a)[34, 35]. Surface-displayed Bim BH3 exhibited strong binding to 100 nM of a soluble construct of Bfl-1 lacking the putative C-terminal trans-membrane domain (Fig. 2b).

Following transformation of the designed library into yeast, we performed fluorescence activated cell sorting (FACS) for four rounds to identify clones that bound to Bfl-1 at 1 μM, and a fifth round of screening at 100 nM Bfl-1 (Fig. 2c). Library populations after rounds 4 and 5 of positive screening did not exhibit binding to antibodies in the absence of Bfl-1, and interaction with Bfl-1 was blocked in the presence of excess unlabeled Bim BH3 (Supplemental Fig 1), supporting binding to the same site.

Next, we used Illumina technology to sequence library pools from rounds 2, 4 and 5 of sorting, and also a pool screened only for successful expression of BH3 peptides on the yeast surface. Sequence logos are shown in Figure 2d. Figure 2e shows the distribution of $PSSM_{Bfl\text{-}1}$ scores for the unselected library, and for populations from rounds 4 and 5. By construction, wild-type Bim BH3 was assigned the highest possible $PSSM_{Bfl\text{-}1}$ score of 0 (see Methods). The $PSSM_{Bfl\text{-}1}$ scores for different pools were consistent with progressive enrichment of the library in high-scoring sequences, and depletion of low scoring sequences, indicating that $PSSM_{Bfl\text{-}1}$ scores were useful for recognizing non-binders and weak binders. For example, despite the library optimization strategy, some residues classified as disruptive were included due to codon choice. In most cases, these were subsequently removed in screening (e.g. Asn at 2d, Asp and His at 3a, Asp and Pro at 3d; Table 1). However, predicted disruptive residues were occasionally found in sequences identified by screening, notably at positions 2e and 2g. Tyr at 2e occurred with high frequency in library binders, contrary to the SPOT-based PSSM predictions. A peptide from round-4 selection with tyrosine at 2e competed with fluorescent Bim BH3 binding to Bfl-1, although weakly compared to wild-type Bim-BH3 (peptide FD3 in Supplemental Fig. 2).

Using the Illumina sequencing data, we tracked the enrichment of individual Bfl-1-binding sequences over successive rounds. Wild-type Bim BH3 and clones FD1 and FD2 (Table 2) were enriched over rounds 2, 4 and 5, and were also found in conventional sequencing of 96 clones from round 4 of screening (sequence logo in Supplemental Fig. 3). We synthesized 23-residue peptides corresponding to Bim BH3, FD1, and FD2, and measured binding to all five pro-survival proteins using a fluorescence polarization assay that involved competition with an 18-residue fluoresceinated Bim BH3 peptide (Table 2; Supplemental Fig. 4). Consistent with the yeast-surface results, both FD1 and FD2 competed strongly with Bim BH3 for binding to Bfl-1 (K_i values in Table 2). The slow off-rate observed for dissociation of a 23-residue Bim BH3 peptide from Bfl-1 and Mcl-1 prevented us from measuring accurate K_i values for these interactions. FD1 bound to all pro-survival proteins strongly, although more weakly to Bcl-2, Bcl-w and Bcl-x_L than to Bfl-1 and Mcl-1. FD2 exhibited ~4-60-fold specificity for Bfl-1 over Bcl-x_L, Bcl-2 and Bcl-w, but bound very tightly to Mcl-1. Overall these results indicated that high affinity Bfl-1 binders could be obtained by screening for interaction with Bfl-1, but the peptides that were identified also bound tightly to Mcl-1 and with variable affinities to other pro-survival proteins.

Competition screening for selective binders of Bfl-1—The yeast population after four rounds of screening for Bfl-1 binding showed significant interaction with all five pro-survival proteins at 100 nM (Supplemental Fig. 5). To identify the most selective binders in this population, we introduced competition into the screening protocol. Bcl-x_L and Mcl-1 represent distinct subclasses of pro-survival proteins in terms of sequence identity and binding specificity, so we screened for Bfl-1-specific BH3 peptides by incubating the round-4 sorted population with labeled Bfl-1 in the presence of 100-fold excess unlabeled Bcl-x_L and Mcl-1 (Figure 3). After three rounds of competition screening, the library clones exhibited improved binding to Bfl-1 compared to both the initial starting population (round 4) and Bim BH3. Sequencing 94 clones from this population gave predominantly one sequence (90 out of 94): FA1 (Table 2). On the surface of yeast, FA1 retained binding to 10 nM Bfl-1 in the presence of 100-fold excess Mcl-1 and Bcl-x_L, in contrast to Bim (Figure 3;

compare b and f). However, FA1 still displayed binding in the low nanomolar range to Mcl-1 and Bcl-x_L on the surface of yeast (Supplemental Fig. 6). Separately, we performed competition screening for binding to Bfl-1 in the presence of excess unlabeled Bcl-x_L or Mcl-1 individually. These screens resulted in pools that were also dominated by clone FA1 (>90%).

In agreement with the PSSM models, we found that most clones from the round-4 population bound to Bcl-w at 100 nM (Supplemental Fig. 5). Therefore, we performed a separate screen for binding to 10 nM Bfl-1 in the presence of excess unlabeled Bcl-w. After two rounds of competition sorting, we isolated clones that did not bind to Bcl-w at 10 nM (negative selection). Sequencing of 19 individual clones from this population resulted in 12 occurrences of sequence FW1 (Table 2: Supplemental Table 2).

We synthesized FA1 and FW1 as fluoresceinated 23-residue peptides. Very tight binding of fluoresceinated FA1 to Bfl-1 and Mcl-1 precluded accurate determination of K_d values using direct binding assays (data not shown). In addition, fluoresceinated FA1 showed extremely slow dissociation from Bfl-1 in solution ($t_{1/2}$ > 30 hours) (Supplemental Table 1). This is probably because the yeast-surface display screening, which is done under non-equilibrium conditions, selects for slow off-rates. Slow binding kinetics mean that solution equilibrium binding measurements would require impractically long incubation times. Therefore, we used bio-layer interferometry to further investigate the kinetics of binding of unlabelled FA1 (no dye) to Bfl-1 (Fig. 4A).

We again observed that the dissociation kinetics of Bfl-1 from surface-bound FA1 were extremely slow. There was no detectable decrease in signal beyond the noise level for more than 1000 seconds, providing an upper limit on k_{off} of ~1.5 × 10–5 s^{-1}.and an upper limit on the K_d of ~0.3 nM. Thus, FA1 is a high-affinity binder of Bfl-1 with a half-life for dissociation of > 12 hours. Dissociation of Mcl-1 and Bcl-x_L from FA1 was faster, allowing us to determine K_d values from bio-layer interferometry of ~6 and ~33 nM for these proteins, respectively (Figure 4A). These data are consistent with FA1 being a selective binder of Bfl-1.

To further quantify the binding of FA1 to the pro-survival proteins, we performed competition experiments with fluoresceinated Bim-BH3 (Table 2: Supplemental Figure 4). Except for the interaction of FA1 with Bfl-1, all mixtures were equilibrated in reasonable times. Unlabeled FA1 competed with Bim-BH3 binding to each pro-survival protein, with varying affinities (K_i values in Table 2). This experiment also indicated that FA1 bound to the same hydrophobic groove as Bim BH3 on each protein.

The extremely slow off-rate for dissociation of FA1 from Bfl-1 made it difficult to quantify the equilibrium binding specificity of this peptide in solution, although our data are consistent with preferential binding to Bfl-1. The slow binding kinetics make the equilibrium binding properties somewhat irrelevant, given that it is highly unlikely that experiments using this reagent would be performed under equilibrium conditions. We have established that FA1 will remain bound to Bfl-1 much longer than to any of the other pro-survival proteins examined here. For possible *in vivo* applications of a Bfl-1 inhibitor, this could be advantageous[36].

We measured the dissociation kinetics of fluoresceinated FW1 in solution and found that, in contrast to FA1, FW1 had faster off rates for both Bfl-1 ($t_{1/2}$ ~37 mins) and Mcl-1 ($t_{1/2}$ ~3 hrs) (Supplemental Table 1). Competition binding studies using unlabeled FW1 showed that this peptide was much more effective at competing with fluoresceinated Bim BH3 for binding to Bfl-1 compared to Bcl-w, with a ~37-fold lower K_i for Bfl-1 compared to Bcl-w (Table 2; Supplemental Figure 4). FW1 bound with sub-nanomolar affinity to Mcl-1, and

with 20 – 30 nM affinity to Bcl-x_L and Bcl-2, consistent with the screening protocol, which included only Bcl-w as a competitor.

Modulating the affinity and specificity of FA1 through mutation—FA1 is a high-affinity binder of Bfl-1 with a very slow dissociation rate. Its slow off-rate made it difficult to analyze determinants of its binding specificity. We thus introduced a point mutation into FA1 that adjusted its affinity into the range of many BH3 peptides derived from native proteins[18, 22]. Aspartate at position 3f is conserved in all natural BH3 proteins, and SPOT arrays indicated that mutating this residue reduces binding to all receptors (which is why it was not included in the screen)[31, 32]. We introduced the mutation D3fK into FA1 (FA1_D3fK). The mutant naming convention here and below indicates the original residue, the BH3 position that is the site of the substitution (as labeled in Fig. 1a), then the mutated residue. Similar to FA1, FA1_D3fK competed with fluorescent Bim BH3 for binding to Bfl-1, although at higher concentration compared to FA1 (Supplemental Fig. 7). We determined that dye-labeled FA1_D3fK had a much faster off-rate for Bfl-1 ($t_{1/2}$ ~ 5 minutes: Supplemental Table 1), so binding to all five receptors could be more readily quantified.

FA1_D3fK bound to Bfl-1 with a K_d of ~47 nM, but bound to all the other receptors with K_d > 1 μM (Figure 4B). Thus, FA1_D3fK is selective for Bfl-1.

There are three substitutions in FA1 compared to Bim: I3dA, E3gV and F4aL. We quantified the contributions of the individual mutations to binding specificity in the context of Bim_D3fK (Figure 4c). We first tested the influence of D3fK, which itself does not confer specificity for Bfl-1 over Mcl-1 and Bcl-x_L. Interestingly, this mutation provides moderate specificity against Bcl-w. Asp at 3f in Bim BH3 interacts with a salt bridge triad consisting of Asp 81, Asn 85 and Arg 88 (human Bfl-1 numbering) in several Bfl-1 structures[27, 28]. Interestingly, Asp 81 in Bfl-1 is conserved between Bfl-1, Mcl-1, Bcl-x_L and Bcl-2, but not Bcl-w, which has a deletion at this site relative to other family members (Fig. 5 a–c). Absence of a favorable electrostatic interaction between the introduced Lys and Asp 81 may explain why the D3fK substitution destabilizes binding to Bcl-w more than to other pro-survival proteins.

In the context of Bim_D3fK, I3dA significantly destabilized binding to Mcl-1, consistent with SPOT arrays and previous observations that substitution at 3d in Bim-BH3 is not well tolerated for Mcl-1 binding[31, 32]. In contrast, Bfl-1, Bcl-x_L, Bcl-2 and Bcl-w tolerate a broad range of substitutions at the I3d position[30, 32]. This tolerance may arise from small structural adjustments that are possible in the α2/α3 region of the binding groove of these proteins, near peptide position 3d[37]. Fire et al. described variation in structures of Bcl-x_L bound to different peptides around this site[38], and Smits et al. described small variations in the interactions of different peptides with Bfl-1[28]. It is also interesting that Ile at Bim BH3 position 3d occupies a preferred rotamer when bound to Mcl-1 (rotamer probability 81% in helices[39]; PDB 2PQK[38]), which strongly prefers Ile at this site. But this residue is found in low-probability rotamers in complexes with Bfl-1 (1% rotamer probability; PDB 2VM6[27]) and Bcl-x_L (4% rotamer probability; PDB 3FDL[40]) This indicates some frustration at this site, which may offset favorable hydrophobic interactions made by Ile with these proteins, thereby minimizing the penalty of mutation from Ile to other residues.

Leucine at position 4a in Bim_D3fK stabilized binding to Mcl-1 and Bfl-1, relative to Bcl-x_L and Bcl-w, thereby providing specificity against Bcl-x_L and Bcl-w at the expense of specificity against Mcl-1. Mcl-1 is known to be highly tolerant to mutations at this site in Bim BH3, and substitution of Phe with Val in Bim BH3 at 4a stabilizes binding to Mcl-1[31]. Structures of Bim BH3 and Puma BH3 bound to Bfl-1 allow a comparison of the

interactions of Phe and Leu at 4a[28]. As shown in Fig. 5d and 5e, the Leu residue of Puma can fill an additional Bfl-1 pocket that is not accessible to Phe, likely explaining the stabilizing effect of the Phe-to-Leu mutation in Bim D3fK.

The E3gV substitution did not significantly affect binding to any pro-survival protein in the context of D3fK. We measured a modest 2.5-fold weakening of binding to Bcl-w and a modest 2-fold increase in binding to Bfl-1. There is a glutamate residue at position 47 of Bfl-1, very near the Bim BH3 3g site, and this residue is conserved as arginine in Bcl-x_L, Bcl-2 and Bcl-w (Fig. 5c). Thus, in peptide FA1, E3gV might confer a preference for Bfl-1 binding via an electrostatic mechanism. Interestingly, four peptides selected to be specific for Bfl-1 over Bcl-w (FW2, FW3, FW4 and FW6) had a lysine substitution at 3g. Finally, in a previous study(*3*), substitution of lysine with glutamate at 3g in Noxa conferred binding to Bcl-x_L and Bcl-w. Thus it appears that mutation of glutamate at position 3g may sometimes contribute to a preference for binding Bfl-1.

PSSM predictions

We analyzed the results of our library design and experimental screening according to predictions of the PSSM model. $PSSM_{Bfl\text{-}1}$ scores for all sequences in the library, and for binders identified from screening, were strongly correlated with PSSM scores for binding to the other pro-survival proteins Mcl-1, Bcl-x_L, Bcl-2 and Bcl-w (Fig. 1e – h and Fig. 6a, b). This indicates that most of the Bim BH3 sequence changes that satisfied our library design requirements were predicted to have similar effects on many of the interactions. Experimental binding profiles for yeast library populations after 4 or 5 rounds of sorting supported a correlation of binding strengths, because clones selected for binding to Bfl-1 also exhibited significant binding to Mcl-1, Bcl-x_L and Bcl-w at 100 nM (Supplemental Fig. 5).

Sequences obtained after screening only for binding (described by the logo in Fig. 2d) show that all variable sites, including the boundary positions 2e, 2g and 3g, were occupied at high frequency by large and/or hydrophobic residues. Competitive binding with Bim BH3 indicated that yeast-displayed peptides with these sequences bound specifically to the same site on Bfl-1 (Supplemental Fig. 1). Large hydrophobic residue substitutions were predicted to be favorable according to the SPOT array (Fig. 1c), but polar residues such as Arg, Lys, Ser, Thr and Gln also had good $PSSM_{Bfl\text{-}1}$ scores yet were not observed with high frequency. When we imposed a requirement for tighter binding to Bfl-1 and specific binding to Bfl-1 over other pro-survival proteins (Mcl-1 and Bcl-x_L, or Bcl-w), we isolated FA1 and FW1 (Table 2). For FA1, position 2g was selected as Glu, rather than as one of the predominant Phe/Trp/Val/Ile residues found after only positive screening, and FW1 had Gly at this position. All three mutations observed in clone FA1 were predicted to be specific over Mcl-1, Bcl-x_L and Bcl-2 according to the PSSMs: Ala at 3d over Mcl-1; Val at 3g over Mcl-1, Bcl-x_L and Bcl-2; Leu at 4a over Bcl-x_L (Table 1).

Very few experimentally identified binders had $PSSM_{Bfl\text{-}1}$ scores of less than −1.7 (Fig. 2d, Fig. 6). But many sequences that were predicted to have high Bfl-1 scores (> −1) and lower Mcl-1 or Bcl-x_L scores (< −2), i.e. sequences scored in the off-diagonal, lower right side in Figures 6a and b, did not appear among clones screened for Bfl-1 binding. Most sequences in this region had Asn at 3a, and this mutation was not recovered in our screen. The model also predicted that Lys/Tyr at position 2d and Ser at position 3d would provide specificity over Mcl-1, and Lys/Arg at position 4a would provide specificity over Bcl-x_L, but these residues were either absent or present at a very low frequency after positive selection. Illumina sequencing of expression-positive library cells (Fig. 2d) did not indicate any bias against these residues prior to screening. Further studies would be required to determine

whether the PSSM predictions are incorrect or whether aspects of the screen, or the sequence context of the best binders, disfavored selection of these mutations.

Conclusions

The space of possible BH3-like peptide sequences is vast, so systematically uncovering sequence-binding relationships in this protein family is challenging. We have carried out several studies looking at how sequence variation in Bim BH3 influences binding to different pro-survival proteins[31, 32, 43]. The approach we present here, combining SPOT array-guided computational design with experimental screening, was chosen to focus experimental studies into interesting parts of the sequence space. We successfully identified new BH3-like partners for Bfl-1, particularly the slowly-dissociating FA1 and the selective binder FA1_D3fK. Our design strategy can be generalized to other Bcl-2 family complexes and other types of protein-protein interaction systems and will lead to a better understanding of binding specificities. In addition, peptides identified in this work hold potential to be used as reagents for studying apopototic regulation.

Methods

PSSM model derived from SPOT array experiments

As previously described[31], the PSSM score for amino acid i at position j binding to a specific pro-survival protein R, S(Ri,j), was obtained by taking the logarithm ($\log_{10}$) of the ratio of the fluorescence intensity for the corresponding Bim BH3 point mutant to the intensity of wild-type Bim BH3 (averaged over all wild-type spots) on the membrane.

Bfl-1 library design

For library design of Bfl-1, the Bfl-1 PSSM model was obtained by averaging the PSSM scores derived from membranes probed with 100 nM and 1 μM of Bfl-1. The PSSM model for Bcl-2 was obtained by the same procedure, and the model for Bcl-w was derived from a membrane probed with 100 nM Bcl-w only[31]. PSSM models for Bcl-x_L and Mcl-1 were described previously (we used the improved PSSM model using library SPOT arrays in Dutta et al.[31]). Normalized intensities with values greater than 1 were capped at 1 before deriving PSSM scores. The definition of non-disruptive residues and 4 different types of specific residues is given in the Results. For a residue to be defined as specific, the difference between its Bfl-1 PSSM score and its score for another receptor was required to be larger than $\log_{10}(1.5)$, and the residue also had to be in the top 33% when ranked by PSSMBfl-1 – PSSMX for some X, where X is Bcl-xL, Mcl-1, Bcl-2 or Bcl-w. The native residue was classified as both a non-disruptive and a specific residue for purposes of library design. Because Met and Cys substitutions were not included on the membrane, their scores were defined as those of Leu and Ser, respectively, when predicting non-disruptive residues. However, these residues were not scored for the specificity predictions. In addition, Pro was removed from consideration as a specific residue. Four quantities were defined for each degenerate codon j at position i: (1) the size, s_{ij}, which is the number of unique tri-nucleotides within the codon, (2) nd_{ij}, the number of non-disruptive residues encoded by the codon, (3) sp_{ij}, the number of specific residues (considering all 4 different types) encoded by the codon, and (4) m_{ij}, the number of “misses” in chemical diversity for the codon. The metric m_{ij} was defined for codons at positions 2d, 2g, 2e, 3b, 3a, 3d, 4a. Amino acids were divided into different classes according to their physicochemical properties, and the number of classes with no representation among the amino acids encoded by the codon was counted. For the more buried positions 2d, 3a, 3d, 4a, the classes were [A], [L], [IV], [FY]. For the more exposed positions 2g, 3b, 3g, the classes were [AG], [DE], [KR], [NQ], [ST]. A “miss” was scored for a class only if at least one amino acid from that class was designated non-

disruptive. A codon was considered more chemically diverse if it had a lower m_{ij}. At each designed position, we only considered degenerate codons that encoded (1) the native Bim BH3 amino acid and (2) at least one of each type of specific residue at that position (not counting the native residue as a specific residue). The set of remaining degenerate codons was trimmed further by comparing every pair of codons. If a degenerate codon had a larger s_{ij}, a smaller sp_{ij}, and a larger m_{ij} than another codon, then the first codon was considered dominated by the second and was eliminated from the pool. The elimination process was repeated until no degenerate codon dominated any other codon in the remaining set. Optimization of degenerate codon combinations, out of the remaining pool of codons D_i at each designed position i, was performed by solving the following integer linear programming problem:

$$\text{Max } \Sigma i \Sigma j \in D_i \, c_{ij} \log(nd_{ij}) + \Sigma i \Sigma j \in D_i \, c_{ij} \log(sp_{ij})$$

$$\text{subject to } \Sigma i \Sigma j \in D_i \, c_{ij} \log(s_{ij}) <= 7$$

$$\text{subject to } \Sigma i \Sigma j \in D_i \, c_{ij} \, m_{ij} <= 4$$

$$\text{subject to } \Sigma j \in D_i \, c_{ij} = 1 \text{ for each position i}$$

Where $c_{ij} = 1$ if codon j was picked at position i, and 0 otherwise. For the winner codon j picked at each position i, $\Sigma_i \log(nd_{ij}) = \log(\Pi_i nd_{ij})$ is the logarithm of the number of unique protein sequences encoded with all designed positions occupied by non-disruptive residues, $\Sigma_i \log(sp_{ij}) = \log(\Pi_i sp_{ij})$ is the logarithm of the number of unique protein sequences encoded with all designed positions occupied by specific residues, and $\Sigma_i \log(s_{ij}) = \log(\Pi_i s_{ij})$ is the logarithm of the library size (or the number of unique DNA sequences in the library) as described in the text. $\Sigma_i m_{ij}$ is the total number of misses in chemical diversity across all positions and we manually picked 4 as a threshold. The problem was solved using the glpsol solver in the GLPK package (GNU MathProg).

Expression and purification of pro-survival proteins

All pro-survival proteins were purified as described previously, and the constructs used were the same as in that work[31, 32].

Library construction—Construction of the yeast display vector used in this study was described previously[31]. The combinatorial library was constructed using homologous recombination in yeast. The wild-type Bim-BH3 gene was randomized using the mutagenic forward primer (5' GGCCGTCCGGAAATTTGG WWK BMT CAG DDK VWC CGT CGT NNT GGC GAT VHA WDK AATGCGTATTATGCGCGTCGC 3'; N represents a mixture of A, T, G and C; W represents a mixture of A and T; K represents a mixture of G and T; B represents a mixture of C, G and T; M a mixture of A and C; D represents a mixture of A, G and T; V represents a mixture of A, C and G; H represents a mixture of A, C and T;) and a reverse primer (5' CTAAAAGTACAGTGGGAACAAAGTCG 3'). The PCR product was further extended at the 5' end to provide overlapping ends of more than 50 base pairs to increase transformation efficiency[44]. The amplified product was purified using a PCR purification kit (Qiagen), and transformed into yeast along with an acceptor vector cut with Nhe1 and Xho1. Transformation was done using electroporation following an established protocol[45].

Yeast display and FACS screening—Yeast cells were analyzed in a BD FACScan or BD FacsCalibur flow cytometer powered by CellQuest software. For the first five rounds of positive sorting against myc- tagged Bfl-1, yeast library cells were prepared and labeled as described previously[31]. Library cells after 4 rounds of positive sorting were further sorted for specific binding to Bfl-1 using competition. For competition sorts, all pro-survival proteins (tagged Bfl-1 and untagged competitors) were first mixed together and then added

to the cells. To sort cells displaying peptides specific for Bfl-1 over Bcl-x_L and Mcl-1, 2 × 10^7 library yeast cells from the 4th round were mixed with 100 nM Bfl-1 in the presence of 500 nM of His-tagged Bcl-x_L and 500 nM untagged Mcl-1 in 50 mM Tris, 100 mM NaCl pH 8.0. Mixtures were incubated for at least 2 hours. All subsequent steps were performed with ice-cold buffer. After washing off unbound receptor with the same buffer, cells were labeled with primary antibodies (anti-FLAG rabbit and anti-c-myc mouse) (Sigma) followed by washing and labeling with secondary antibodies (fluorescein (FITC)-conjugated goat anti-rabbit antibody and R-Phycoerythrin (PE)-conjugated goat anti-mouse IgG (Sigma) or an allophycocyanin (APC) labeled goat anti-mouse IgG (BD Biosciencecs)). In the first round of competition selection, ~1% of the expression positive population was collected. In subsequent rounds, incubation was done with 10 nM Bfl-1 in the presence of 500 nM Bcl-x_L and 500 nM Mcl-1, and the sorting gate was reduced to collect 0.2–0.5% of the expression-positive population. For competition screens against only Bcl-x_L or only Mcl-1, a similar protocol was followed except that library yeast cells from the 4th round were mixed with 100 nM Bfl-1 in the presence of either 500 nM of His-tagged Bcl-x_L or 500 nM untagged Mcl-1 separately, and the top ~1–2% of the expression-positive population was collected. Two subsequent competition screens were done in the presence of 10 nM Bfl-1 and 500 nM Bcl-x_L or 500 nM Mcl-1. For Bcl-x_L, one further round was performed in the presence of 10 nM Bfl-1 and 1 μM Bcl-x_L. Two rounds of competition screening including Bcl-w were performed with the round-4 population, using 10 nM Bfl-1 in the presence of 10 μM untagged Bcl-w. To further eliminate Bcl-w binding peptides, we followed the competition sorts with a negative sort for cells that did not bind to 10 nM Myc-tagged Bcl-w. Analysis of the library population for binding to different pro-survival proteins was performed using FITC fluorescence for expression and APC fluorescence to observe binding. Sorting of yeast cells was performed in a BD FacsAria or Cytomation MoFlo using 488 nm and/or 561 nm excitation.

Peptide synthesis and biotinylation—All unlabelled and fluoresceinated peptides were synthesized by the MIT Biopolymers Laboratory. Fluoresceinated Bim–BH3 used for fluorescence polarization was 18 residues long. All other Bim BH3 peptides variants used in this study were 23 residues long. Peptides were purified using reverse phase HPLC with a C18 column and a linear water/acetonitrile gradient. Peptides for fluorescence polarization binding assays had N-acetylated and C-amidated ends, with the exception of FD2, which had free ends for improved solubility. For bio-layer interferometry, peptide FA1 (23 residues) was synthesized with a free N terminus and an amidated C-terminus and biotinylated using the EZ-link NHS-PEG4-biotin from Thermo Scientific using the manufacturer's protocol. The biotinylation reaction was performed at room temperature for 30–60 minutes, following which the biotinylated peptide was purified using reverse phase HPLC with a C18 column. The mass of the biotinylated peptide was confirmed by mass spectrometry.

Bio-layer interferometry studies—All experiments were performed using the BLITZ system from ForteBio. Biotinylated FA1 at a concentration of 0.1 mg/ml was captured on Streptavidin (SA) biosensors (ForteBio) to levels of ~0.42 response units. Pro-survival proteins Bfl-1, Mcl-1 and Bcl-x_L, at 2–3 concentrations ranging from 30–250 nM, were bound to FA1 for 10 minutes and then allowed to dissociate in phosphate buffer (20 mM phosphate, 50 mM sodium chloride, 0.1% BSA, pH 7.5). Dissociation was monitored over 60 minutes for Bfl-1 and Mcl-1 and over 10 minutes for Bcl-x_L. From the dissociation phase data for Bfl-1 binding, an upper bound on the off-rate was estimated from the fluctuation in signal over 1000 seconds. Dissociation phase data for Mcl-1 and Bcl-x_L were fit to the reaction $RU_t = Aexp(-k_{off}t) + RU_{base}$ where RU_t is the observed response unit, A is the amplitude of the signal, k_{off} is the rate constant for dissociation, t is the time and RU_{base} is

an added parameter to account for change in baseline after dissociation of the ligand[46]. All three parameters A, k_{off} and RU_{base} were fit. The association phase was fit to the equation $RU_t = RU_{base} + Ck_{on}R_{max}[1\text{-}exp(-B_t)]/B$ where $B = Ck_{on}+k_{off}$, RU_t is the observed response units, C is the concentration of the pro-survival protein, k_{on} is the on rate constant, k_{off} is the off rate constant, R_{max} is the capacity of the peptide immobilized on the biosensor. The three parameters RU_{base}, k_{on} and R_{max} were fit, and off-rate parameters were taken from the dissociation analysis. Analysis of kinetic data was performed using Igor Pro 6.02A (Wavemetrics).

Fluorescence polarization binding assays—Both direct and competition binding assays were done at 37 ºC in 20 mM sodium phosphate, 50 mM NaCl, 1 mM ethylenediaminetetraacetic acid, 0.001% triton X (v/v), and 5% DMSO (v/v), pH 7.8]. Concentrations of labeled and unlabeled peptides are given in Table 2. The dissociation half-lives of fluorescently labeled peptides for different pro-survival proteins (reported in Supplementary Table 1) were measured by monitoring the decrease in anisotropy with time after addition of excess unlabeled Bim (1 μM) to a premixed solution of 10–20 nM of fluoresceinated peptide with 50–100 nM of individual pro-survival proteins. Data were fit to a single exponential given by the equation $RU_t = Aexp(-k_{off}t) + RU_{base}$ as described above. For direct-binding assays, pro-survival proteins were first serially diluted in a 96-well plate followed by the addition of the fluorescently labeled peptides. The plates were incubated at 37 °C for 4–6 hours before reading. For competition binding assays, unlabeled peptides and fluorescently labeled peptides were incubated for 10 minutes before the relevant pro-survival protein was added to the mixture. The plates were incubated at 37 ºC and the anisotropy monitored over a time period of 4–24 hours. Due to the extremely slow off rates observed for the 23-mer Bim-BH3 peptide for Bfl-1 and Mcl-1 and for 23-mer FA1 for Bfl-1, we do not report K_i values for these interactions. However, we did not observe any significant change in anisotropy after 4 hours of incubation. Measurements with longer equilibration times were not reliable due to loss of signal of the free fluorescent peptide over time. Direct binding data were fit to a model for single-site binding as described previously[47]. Competition binding data were fit to a model that considered depletion of the labeled and unlabeled peptide as described previously[31, 48]. Curve fitting was performed using the program Igor Pro 6.02A (Wavemetrics).

Illumina sequencing of library pools—Illumina sample preparation and data analysis were described previously[32]. Briefly, DNA was extracted from yeast library cells using Zymoprep Yeast Plasmid Miniprep I kit (Zymoresearch). Following PCR amplification using High Fidelity Taq DNA polymerase (Invitrogen), the product was purified using the Qiagen PCR purification kit. Sample purity was checked using the Agilent 2100 BioAnalyzer at the MIT BioMicro Center. Sequencing was performed using the Illumina HiSeq system. Only sequences with Illumina quality scores with an overall confidence of 0.995 over all the variable nucleotides in a read were considered. For sequence logo construction in Figure 2, only unique sequences that occurred 20 or more times in each library pool after 2, 4 and 5 rounds of positive screening were included.

Supplementary Material

Refer to Web version on PubMed Central for supplementary material.

Acknowledgments

We thank the Imperiali laboratory for the use of their Blitz system for bio-layer interferometry studies, the Koch Institute Biopolymers and Proteomics Facility for peptide synthesis and the Swanson Biotechnology Center Flow Cytometry Facility at MIT for assistance with cell sorting and analysis. We thank L. Reich for preliminary

processing of the Illumina sequencing data and members of the Keating lab for critical reading of the manuscript and valuable suggestions. This work was funded by NIGMS awards GM084181 and P50-GM68762.

References

(1). Leber B, Lin J, Andrews DW. Embedded together: the life and death consequences of interaction of the Bcl-2 family with membranes. Apoptosis. 2007; 12:897–911. [PubMed: 17453159]

(2). Huang DC, Strasser A. BH3-Only proteins-essential initiators of apoptotic cell death. Cell. 2000; 103:839–842. [PubMed: 11136969]

(3). Chen L, Willis SN, Wei A, Smith BJ, Fletcher JI, Hinds MG, Colman PM, Day CL, Adams JM, Huang DC. Differential targeting of prosurvival Bcl-2 proteins by their BH3-only ligands allows complementary apoptotic function. Mol Cell. 2005; 17:393–403. [PubMed: 15694340]

(4). Cory S, Huang DC, Adams JM. The Bcl-2 family: roles in cell survival and oncogenesis. Oncogene. 2003; 22:8590–8607. [PubMed: 14634621]

(5). Beroukhim R, Mermel CH, Porter D, Wei G, Raychaudhuri S, Donovan J, Barretina J, Boehm JS, Dobson J, Urashima M, Mc Henry KT, Pinchback RM, Ligon AH, Cho YJ, Haery L, Greulich H, Reich M, Winckler W, Lawrence MS, Weir BA, Tanaka KE, Chiang DY, Bass AJ, Loo A, Hoffman C, Prensner J, Liefeld T, Gao Q, Yecies D, Signoretti S, Maher E, Kaye FJ, Sasaki H, Tepper JE, Fletcher JA, Tabernero J, Baselga J, Tsao MS, Demichelis F, Rubin MA, Janne PA, Daly MJ, Nucera C, Levine RL, Ebert BL, Gabriel S, Rustgi AK, Antonescu CR, Ladanyi M, Letai A, Garraway LA, Loda M, Beer DG, True LD, Okamoto A, Pomeroy SL, Singer S, Golub TR, Lander ES, Getz G, Sellers WR, Meyerson M. The landscape of somatic copy-number alteration across human cancers. Nature. 463:899–905. [PubMed: 20164920]

(6). Kang MH, Reynolds CP. Bcl-2 inhibitors: targeting mitochondrial apoptotic pathways in cancer therapy. Clin Cancer Res. 2009; 15:1126–1132. [PubMed: 19228717]

(7). Vogler M. BCL2A1: the underdog in the BCL2 family. Cell Death Differ. 19:67–74. [PubMed: 22075983]

(8). Lin EY, Orlofsky A, Berger MS, Prystowsky MB. Characterization of A1, a novel hemopoietic-specific early-response gene with sequence similarity to bcl-2. J Immunol. 1993; 151:1979–1988. [PubMed: 8345191]

(9). Oberdoerffer P, Kanellopoulou C, Heissmeyer V, Paeper C, Borowski C, Aifantis I, Rao A, Rajewsky K. Efficiency of RNA interference in the mouse hematopoietic system varies between cell types and developmental stages. Mol Cell Biol. 2005; 25:3896–3905. [PubMed: 15870264]

(10). Beverly LJ, Varmus HE. MYC-induced myeloid leukemogenesis is accelerated by all six members of the antiapoptotic BCL family. Oncogene. 2009; 28:1274–1279. [PubMed: 19137012]

(11). Riker AI, Enkemann SA, Fodstad O, Liu S, Ren S, Morris C, Xi Y, Howell P, Metge B, Samant RS, Shevde LA, Li W, Eschrich S, Daud A, Ju J, Matta J. The gene expression profiles of primary and metastatic melanoma yields a transition point of tumor progression and metastasis. BMC Med Genomics. 2008; 1:13. [PubMed: 18442402]

(12). Lee CF, Ling ZQ, Zhao T, Fang SH, Chang WC, Lee SC, Lee KR. Genomic-wide analysis of lymphatic metastasis-associated genes in human hepatocellular carcinoma. World J Gastroenterol. 2009; 15:356–365. [PubMed: 19140237]

(13). Senft D, Berking C, Graf SA, Kammerbauer C, Ruzicka T, Besch R. Selective induction of cell death in melanoma cell lines through targeting of Mcl-1 and A1. PLoS One. 2012; 7:e30821. [PubMed: 22292048]

(14). Piva R, Pellegrino E, Mattioli M, Agnelli L, Lombardi L, Boccalatte F, Costa G, Ruggeri BA, Cheng M, Chiarle R, Palestro G, Neri A, Inghirami G. Functional validation of the anaplastic lymphoma kinase signature identifies CEBPB and BCL2A1 as critical target genes. J Clin Invest. 2006; 116:3171–3182. [PubMed: 17111047]

(15). Campone M, Campion L, Roche H, Gouraud W, Charbonnel C, Magrangeas F, Minvielle S, Geneve J, Martin AL, Bataille R, Jezequel P. Prediction of metastatic relapse in node-positive breast cancer: establishment of a clinicogenomic model after FEC100 adjuvant regimen. Breast Cancer Res Treat. 2008; 109:491–501. [PubMed: 17659439]

(16). Olsson A, Norberg M, Okvist A, Derkow K, Choudhury A, Tobin G, Celsing F, Osterborg A, Rosenquist R, Jondal M, Osorio LM. Upregulation of bfl-1 is a potential mechanism of chemoresistance in B-cell chronic lymphocytic leukaemia. Br J Cancer. 2007; 97:769–777. [PubMed: 17726463]

(17). Simmons MJ, Fan G, Zong WX, Degenhardt K, White E, Gelinas C. Bfl-1/A1 functions, similar to Mcl-1, as a selective tBid and Bak antagonist. Oncogene. 2008; 27:1421–1428. [PubMed: 17724464]

(18). Ku B, Liang C, Jung JU, Oh BH. Evidence that inhibition of BAX activation by BCL-2 involves its tight and preferential interaction with the BH3 domain of BAX. Cell Res. 2011; 21:627–641. [PubMed: 21060336]

(19). Werner AB, de Vries E, Tait SW, Bontjer I, Borst J. Bcl-2 family member Bfl-1/A1 sequesters truncated bid to inhibit is collaboration with pro-apoptotic Bak or Bax. J Biol Chem. 2002; 277:22781–22788. [PubMed: 11929871]

(20). Willis SN, Chen L, Dewson G, Wei A, Naik E, Fletcher JI, Adams JM, Huang DC. Proapoptotic Bak is sequestered by Mcl-1 and Bcl-xL, but not Bcl-2, until displaced by BH3-only proteins. Genes Dev. 2005; 19:1294–1305. [PubMed: 15901672]

(21). Zhai D, Jin C, Huang Z, Satterthwait AC, Reed JC. Differential regulation of Bax and Bak by anti-apoptotic Bcl-2 family proteins Bcl-B and Mcl-1. J Biol Chem. 2008; 283:9580–9586. [PubMed: 18178565]

(22). Certo M, Del Gaizo Moore V, Nishino M, Wei G, Korsmeyer S, Armstrong SA, Letai A. Mitochondria primed by death signals determine cellular addiction to antiapoptotic BCL-2 family members. Cancer Cell. 2006; 9:351–365. [PubMed: 16697956]

(23). Tse C, Shoemaker AR, Adickes J, Anderson MG, Chen J, Jin S, Johnson EF, Marsh KC, Mitten MJ, Nimmer P, Roberts L, Tahir SK, Xiao Y, Yang X, Zhang H, Fesik S, Rosenberg SH, Elmore SW. ABT-263: a potent and orally bioavailable Bcl-2 family inhibitor. Cancer Res. 2008; 68:3421–3428. [PubMed: 18451170]

(24). Oltersdorf T, Elmore SW, Shoemaker AR, Armstrong RC, Augeri DJ, Belli BA, Bruncko M, Deckwerth TL, Dinges J, Hajduk PJ, Joseph MK, Kitada S, Korsmeyer SJ, Kunzer AR, Letai A, Li C, Mitten MJ, Nettesheim DG, Ng S, Nimmer PM, O'Connor JM, Oleksijew A, Petros AM, Reed JC, Shen W, Tahir SK, Thompson CB, Tomaselli KJ, Wang B, Wendt MD, Zhang H, Fesik SW, Rosenberg SH. An inhibitor of Bcl-2 family proteins induces regression of solid tumours. Nature. 2005; 435:677–681. [PubMed: 15902208]

(25). Zhai D, Jin C, Satterthwait AC, Reed JC. Comparison of chemical inhibitors of antiapoptotic Bcl-2-family proteins. Cell Death Differ. 2006; 13:1419–1421. [PubMed: 16645636]

(26). Brien G, Debaud AL, Bickle M, Trescol-Biemont MC, Moncorge O, Colas P, Bonnefoy-Berard N. Characterization of peptide aptamers targeting Bfl-1 anti-apoptotic protein. Biochemistry. 2011; 50:5120–5129. [PubMed: 21563784]

(27). Herman MD, Nyman T, Welin M, Lehtio L, Flodin S, Tresaugues L, Kotenyova T, Flores A, Nordlund P. Completing the family portrait of the anti-apoptotic Bcl-2 proteins: crystal structure of human Bfl-1 in complex with Bim. FEBS Lett. 2008; 582:3590–3594. [PubMed: 18812174]

(28). Smits C, Czabotar PE, Hinds MG, Day CL. Structural plasticity underpins promiscuous binding of the prosurvival protein A1. Structure. 2008; 16:818–829. [PubMed: 18462686]

(29). Day CL, Chen L, Richardson SJ, Harrison PJ, Huang DC, Hinds MG. Solution structure of prosurvival Mcl-1 and characterization of its binding by proapoptotic BH3-only ligands. J Biol Chem. 2005; 280:4738–44. [PubMed: 15550399]

(30). London N, Gulla S, Keating AE, Schueler-Furman O. In silico and in vitro elucidation of BH3 binding specificity toward Bcl-2. Biochemistry. 2012; 51:5841–5850. [PubMed: 22702834]

(31). Dutta S, Gulla S, Chen TS, Fire E, Grant RA, Keating AE. Determinants of BH3 binding specificity for Mcl-1 versus Bcl-xL. J Mol Biol. 2010; 398:747–762. [PubMed: 20363230]

(32). DeBartolo J, Dutta S, Reich L, Keating AE. Predictive Bcl-2 family binding models rooted in experiment or structure. J Mol Biol. 2012; 422:124–144. [PubMed: 22617328]

(33). Eilers PH, Goeman JJ. Enhancing scatterplots with smoothed densities. Bioinformatics. 2004; 20:623–628. [PubMed: 15033868]

(34). Boder ET, Wittrup KD. Yeast surface display for screening combinatorial polypeptide libraries. Nat Biotechnol. 1997; 15:553–557. [PubMed: 9181578]

(35). Gai SA, Wittrup KD. Yeast surface display for protein engineering and characterization. Curr Opin Struct Biol. 2007; 17:467–473. [PubMed: 17870469]

(36). Tummino PJ, Copeland RA. Residence time of receptor-ligand complexes and its effect on biological function. Biochemistry. 2008; 47:5481–5492. [PubMed: 18412369]

(37). Liu X, Dai S, Zhu Y, Marrack P, Kappler JW. The structure of a Bcl-xL/Bim fragment complex: implications for Bim function. Immunity. 2003; 19:341–352. [PubMed: 14499110]

(38). Fire E, Gullá S, Grant RA, Keating AE. Mcl-1- Bim complexes accommodate surprising point mutations via minor structural changes. Protein Sci. 2010; 19:507–519. [PubMed: 20066663]

(39). Lovell SC, Word JM, Richardson JS, Richardson DC. The penultimate rotamer library. Proteins. 2000; 40:389–408. [PubMed: 10861930]

(40). Lee EF, Sadowsky JD, Smith BJ, Czabotar PE, Peterson-Kaufman KJ, Colman PM, Gellman SH, Fairlie WD. High-resolution structural characterization of a helical alpha/beta-peptide foldamer bound to the anti-apoptotic protein Bcl-xL. Angew Chem Int Ed Engl. 2009; 48:4318–4322. [PubMed: 19229915]

(41). Hinds MG, Lackmann M, Skea GL, Harrison PJ, Huang DC, Day CL. The structure of Bcl-w reveals a role for the C-terminal residues in modulating biological activity. Embo J. 2003; 22:1497–1507. [PubMed: 12660157]

(42). Holm L, Rosenstrom P. Dali server: conservation mapping in 3D. Nucleic Acids Res. 38:W545–549. [PubMed: 20457744]

(43). Chen TS, Palacios H, Keating AE. Structure-Based Redesign of the Binding Specificity of Anti-Apoptotic Bcl-x(L). J Mol Biol. 2013; 425:171–185. [PubMed: 23154169]

(44). Raymond CK, Pownder TA, Sexson SL. General method for plasmid construction using homologous recombination. Biotechniques. 1999; 26:134–138. 140–141. [PubMed: 9894602]

(45). Chao G, Lau WL, Hackel BJ, Sazinsky SL, Lippow SM, Wittrup KD. Isolating and engineering human antibodies using yeast surface display. Nat Protoc. 2006; 1:755–768. [PubMed: 17406305]

(46). O'Shannessy DJ, Brigham-Burke M, Soneson KK, Hensley P, Brooks I. Determination of rate and equilibrium binding constants for macromolecular interactions using surface plasmon resonance: use of nonlinear least squares analysis methods. Anal Biochem. 1993; 212:457–468. [PubMed: 8214588]

(47). Cushing PR, Fellows A, Villone D, Boisguerin P, Madden DR. The relative binding affinities of PDZ partners for CFTR: a biochemical basis for efficient endocytic recycling. Biochemistry. 2008; 47:10084–10098. [PubMed: 18754678]

(48). Roehrl MH, Wang JY, Wagner G. A general framework for development and data analysis of competitive high-throughput screens for small-molecule inhibitors of protein-protein interactions by fluorescence polarization. Biochemistry. 2004; 43:16056–16066. [PubMed: 15610000]

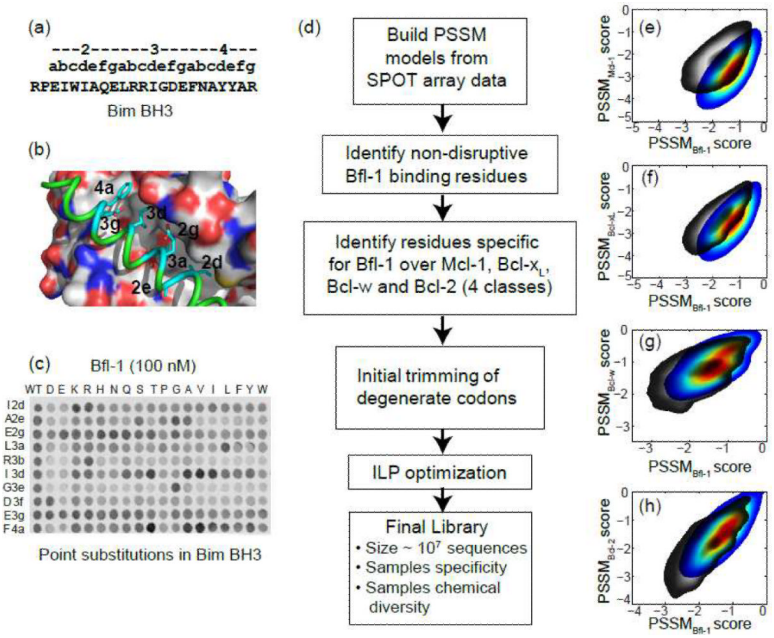

Figure 1.

Computational library design. (a) Bim BH_3 with residue numbering using a heptad convention. (b) Bim BH_3 in complex with Bfl-1 (PDB ID: 2VM6)[27]. Bfl-1 is shown in surface representation colored by atom type. Side chains of residues on Bim BH_3 that were randomized in the library are shown as sticks. (c) Substitution SPOT array image of Bim BH3 point mutants binding to 100 nM Bfl-1[32]. The rows indicate the substituted positions and the columns indicate mutations. The leftmost column corresponds to Bim BH_3. (d) Steps in the procedure for designing a library of peptides to target Bfl-1 in preference to other pro-survival proteins. (e–f) Correlation of $PSSM_{Bfl\text{-}1}$ scores for library sequences with scores from (e) $PSSM_{Mcl\text{-}1}$, (f) $PSSM_{Bcl\text{-}xL}$, (g) $PSSM_{Bcl\text{-}w}$ and (h) $PSSM_{Bcl\text{-}2}$ shown as contour plots for the computationally designed library (color) and the manually designed library of Dutta et al.[31] (gray). The plots were generated using a smoothing routine in MATLAB[33].

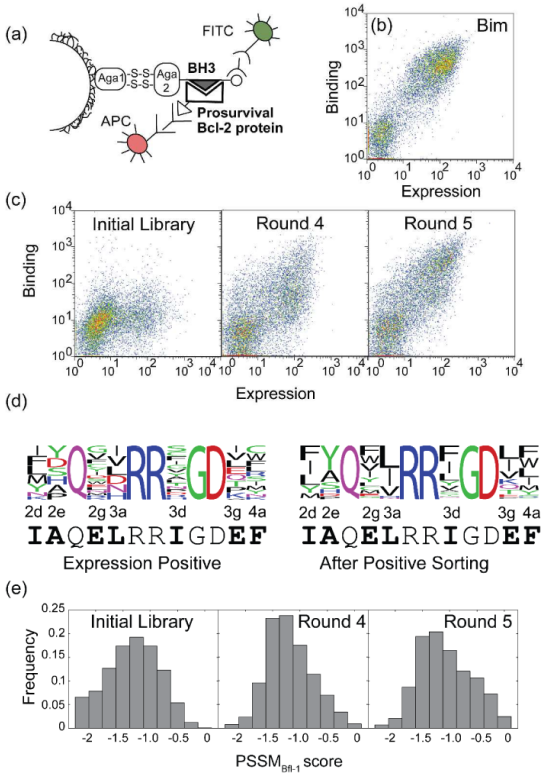

Figure 2.

Yeast-surface display screening to obtain BH_3 peptides that bind to Bfl-1. (a) Schematic of the yeast-surface display system used to screen a BH_3 peptide library. BH_3 peptides were expressed as fusions to the yeast cell surface protein Aga2 and detected using FITC fluorescence. Binding to Myc tagged Bfl-1 was monitored using APC fluorescence. (b) Strong binding of surface displayed Bim-BH_3 peptide to 100 nM Bfl-1 illustrated by the correlation between FITC fluorescence (expression axis) and APC fluorescence (binding axis). (c) Enrichment of Bfl-1 binding to the yeast library through successive rounds of cell sorting. FACS plots of different populations are shown binding to 100 nM Bfl-1. (d) Sequence logo for clones obtained from Illumina sequencing of yeast cells that were expression positive or present at least twenty times in each of positive selection rounds 2, 4 and 5. The numbering of the randomized positions and the wild-type sequence are shown at the bottom. (e) Distribution of $PSSM_{Bfl\text{-}1}$ scores for the entire theoretical library and the library after two different stages of screening. Wild-type Bim BH_3 has the highest possible PSSM score of 0.

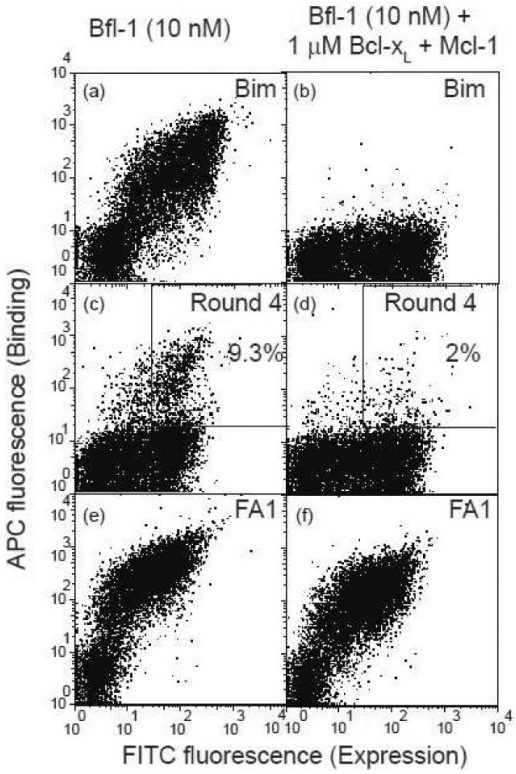

Figure 3.

FACS tests for specific binding to Bfl-1. FACS profiles for Bfl-1 binding to Bim BH_3 (a and b), the library after four rounds of positive selection for Bfl-1 (c and d), or clone FA1 (e and f). Bfl-1 was at 10 nM. Analysis was without (left, panels a, c, e) or with (right, panels b, d, f) 500 nM each of unlabeled Bcl-x_L and Mcl-1. Cell populations displaying BH3 peptides that showed preferential binding to Bfl-1 over Bcl-x_L and Mcl-1 are quantified as a percentage of the total population in panels c and d.

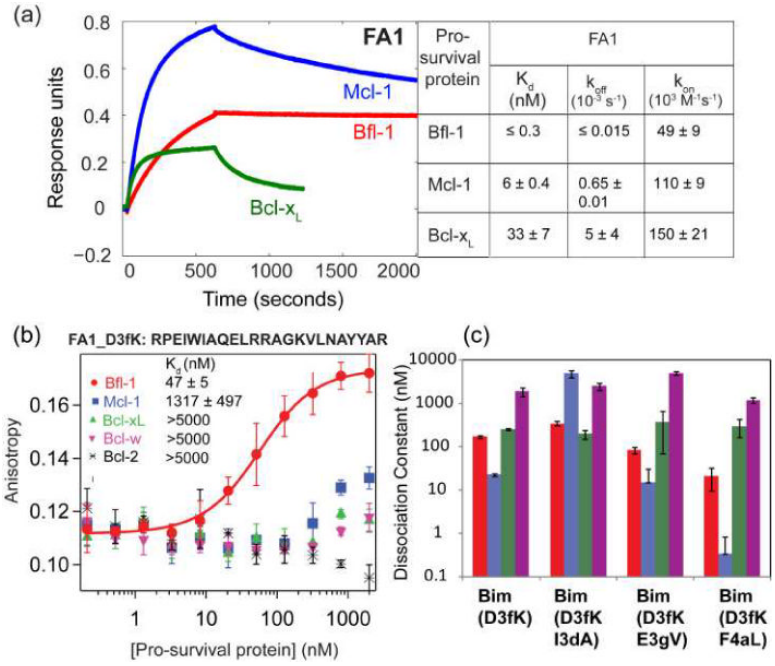

Pro-survival protein	FA1		
	K_d (nM)	k_{off} (10^{-3} s^{-1})	k_{on} (10^3 $M^{-1}s^{-1}$)
Bfl-1	≤ 0.3	≤ 0.015	49 ± 9
Mcl-1	6 ± 0.4	0.65 ± 0.01	110 ± 9
Bcl-x_L	33 ± 7	5 ± 4	150 ± 21

Figure 4.

Equilibrium and kinetic binding data for engineered BH_3 peptides. (a) Kinetic analysis of peptide FA1 binding to Bfl-1, Mcl-1 and Bcl-x_L proteins using the BLITZ bio-layer interferometry system. The peptide was immobilized to a streptavidin biosensor through a biotin at the amino terminus. The protein concentration was 62.5 nM for all three experiments. Errors represent standard deviations from the mean of three independent experiments. (b) Direct binding of fluorescently labeled FA1_D3fK to Bfl-1, Mcl-1, Bcl-x_L, Bcl-w and Bcl-2. The sequence of FA1_D3fK is shown at the top. The concentration of fluoresceinated FA1_D3fK was 10 nM. Average K_d values from a minimum of three experiments are shown with errors corresponding to the standard deviations over replicates. (c) The dissociation constants of different mutants of Bim BH3 for binding to Bfl-1 (red), Mcl-1 (blue), Bcl-x_L (green) and Bcl-w (purple) are shown. The mutations are shown at the bottom.

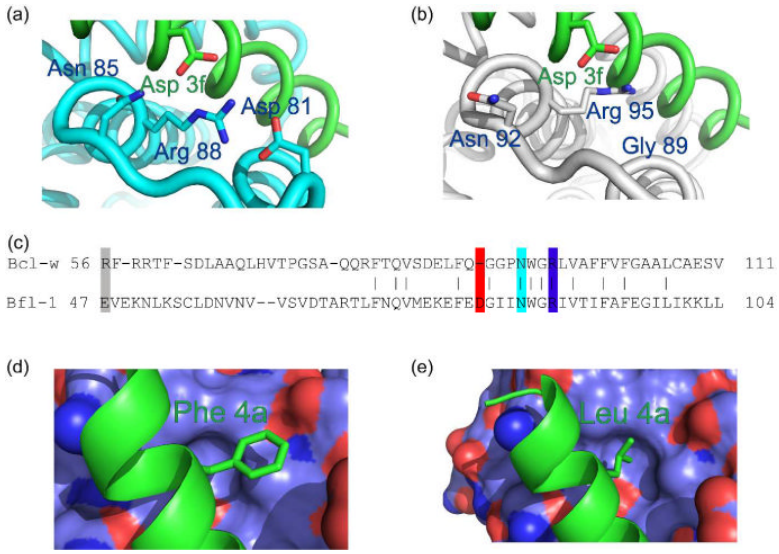

Figure 5.

(a) Electrostatic interactions between aspartate at position 3f of Bim BH_3 (green) with residues Asp 81, Asn 85 and Arg 88 in Bfl-1 (cyan) in the human Bfl-1: Bim (PDB code 2VM6[27]). (b) Structural alignment of Bcl-w (PDB code 1O0L[41]) with the Bfl-1: Bim complex shown in (a). Bfl-1 is omitted for clarity. The corresponding residues are labeled as in (a) to emphasize the missing aspartate. (c) Structure-based sequence alignment using DALI[42] of human Bfl-1 and Bcl-w highlighting the residue changes discussed in the text. Glu 47 in Bfl-1 near the Bim BH_3 3g site is substituted with an Arg in Bcl-w and is shown shaded in grey. (d–e) The hydrophobic pocket surrounding position 4a in the Bim:Bfl-1 structure (PDB code 2VM6[27]) (d) and the Bfl-1: Puma structure (PDB code 2VOF[28]) (e)

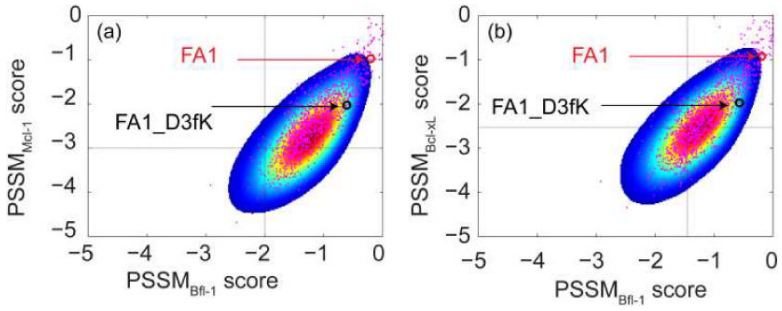

Figure 6.

Distribution of PSSM scores for selected library sequences. (a) Correlation of $PSSM_{Bfl-1}$ with $PSSM_{Mcl-1}$ scores, and (b) $PSSM_{Bfl-1}$ with $PSSM_{Bcl-xL}$ scores. The distribution of scores for the theoretical library is shown as a contour plot[33]. Sequences present at least once in all three library pools from positive screening rounds 2, 4 and 5 were scored for interaction with Bfl-1, Mcl-1 or Bcl-x_L and are shown as points overlaid on top of the contour. Scores for FA1 and FA1_D3fK are shown using red and black circles, respectively.

Table 1

Bfl-1 library design results

	Non-disruptive residues	Specificity		Residues		Residues encoded[a]	Disruptive residues after selection
		vs. Bcl-x_L	vs. Mcl-1	vs. Bcl-2	vs. Bcl-w		
I2d	ACFGHIKMLPRTVWY	-	WKY	-	-	FIKLMNYZ (WWK)	-
A2e	ACGHPS	HS		H	-	ADHPSY (BMT)	Y and D
E2g	ACDEFGHIKNQRSTWY	Y	FGHIKVY	-	GT	CDEFGIKLMNRSVWYZ (DDK)	L and M
L3a	FILMNV	NV	N	N	N	DHILNV (VWC)	-
R3b	AKQR	-	-	-	-	Not randomized	
I3d	ACFGHIMKLNQRSTVY	-	AFGHKNQRSTVY	-	-	ACDFGHILNPRSTVY (NNT)	-
G3e	G	-	-	-	-	Not randomized	
D3f	D	-	-	-	-	Not randomized	
E3g	ACDEFGHIKLMNQRSTVWY	AFHIKLNRQSTVWY	AFILWVY	FIKLRVWY	-	AEIKLPQTV (VHA)	-
F4a	ACFGHIKLMNQRSTVWY	AGHIKLQRSTW	-	K	KR	CFIKLMNRSWYZ (WDK)	-

[a]Disruptive residues included as a result of codon choice are underlined. Codons used for library construction are shown in parentheses

Table 2

Sequences and binding data for natural and engineered BH3 peptides.

Fluorescent Peptide(18 residues)	Sequence			Kd (nM)				
				Bfl-1	Mcl-1	Bcl-x_L	Bcl-w	Bcl-2
Bim	IWIAQELRRIGDEFNAYY			4 ± 1	0.8 ± 0.4	6 ± 1	15 ± 3	5 ± 1
Unlabeled peptides (23 residues)	2	3	4	Ki (nM)				
	defgabcdefgabcdefg							
Bim	RPEIWIAQELRRIGDEFNAYYAR			NE	NE	0.11 ± 0.03	2 ± 0.3	0.8 ± 0.1
FD1	RPEIWLAQYLRRLGDQINAYYAR			0.7 ± 0.2	0.1 ± 0.02	5 ± 0.4	12 ± 3	7 ± 0.8
FD2	RPEIWMAQVLRRFGDLLNAYYAR			3.8 ± 0.7	1 ± 0.1	18 ± 0.2	104 ± 19	223 ± 16
FA1	RPEIWIAQELRRAGDVLNAYYAR			NE	1 ± 0.1	8 ± 0.2	2 ± 1	313 ± 8
FW1	RPEIWIAQGLRRIGDTWNAYYAR			8 ± 2	0.2 ± 0.04	20 ± 4	298 ± 41	31 ± 7

[a] Concentration of fluoresceinated Bim was 10 nM in all experiments.

[b] Concentration of pro-survival protein was 50 nM for competition fluorescence polarization experiments.

[c] Error bars are standard deviations from the mean of a minimum of three experiments.

[a] NE: Not Equilibrated. Ki values are not reported for these interactions due to extremely slow off rates leading to impractically long incubation times to reach equilibrium (see Supplemental Table 2).